GSK3β-Dependent Phosphorylation of the αNAC Coactivator Regulates Its Nuclear Translocation and Proteasome-Mediated Degradation†

Isabelle Quélo,‡ Omar Akhouayri,‡ Josée Prud'homme,‡ and René St-Arnaud*,‡,§

Genetics Unit, Shriners Hospital for Children, Montréal, Québec, Canada H3G 1A6 and Departments of Medicine, Surgery, and Human Genetics, McGill University, Montréal, Québec, Canada H3A 2T5

Received December 16, 2003

ABSTRACT: c-Jun is an immediate-early gene whose degradation by the proteasome pathway is required for an efficient transactivation. In this report, we demonstrated that the c-Jun coactivator, *n*ascent polypeptide associated complex *a*nd *c*oactivator alpha (αNAC) was also a target for degradation by the 26S proteasome. The proteasome inhibitor lactacystin increased the metabolic stability of αNAC in vivo, and lactacystin, MG-132, or epoxomicin treatment of cells induced nuclear translocation of αNAC. We have shown that the ubiquitous kinase glycogen synthase kinase 3β (GSK3β) directly phosphorylated αNAC in vitro and in vivo. Inhibition of the endogenous GSK3β activity resulted in the stabilization of this coactivator in vivo. We identified the phosphoacceptor site in the C-terminal end of the coactivator, on position threonine 159. We demonstrated that the inhibition of GSK3β activity by treatment of cells with the inhibitor 5-iodo-indirubin-3′-monoxime, as well as with a dominant-negative GSK3β mutant, induced the accumulation of αNAC in the nuclei of cells. Mutation of the GSK3β phosphoacceptor site on αNAC induced a significant increase of its coactivation potency. We conclude that GSK3β-dependent phosphorylation of αNAC was the signal that directed the protein to the proteasome. The accumulation of αNAC caused by the inhibition of the proteasome pathway or the activity of GSK3β contributes to its nuclear translocation and impacts on its coactivating function.

The major pathways for protein degradation in cells include lysosomal proteolysis and ubiquitin-dependent as well as -independent proteasomal proteolysis. Lysosomes are predominantly involved in the degradation of internalized extracellular materials and receptors (*1*), whereas ubiquitination regulates the proteolysis of many short-lived and abnormal cellular proteins. A large protein complex, present in both the cytoplasm and the nucleus of cells, called the 26S proteasome, mediates this regulated degradation (*2*−*4*). Within cells, the covalent addition of multiple molecules of ubiquitin targets proteins to the 26S proteasome. The ubiquitin-conjugated proteins are then recognized by the large 19S regulatory complex of the proteasome, and then degraded into short peptides by the 20S proteolytic core complex (*3*, *5*). The 26S proteasome complex is implicated in the proteolysis of many transcription factors (reviewed in ref *6*), including c-Jun (*7*, *8*). In recent years, targeted degradation of transcriptional coactivators via the proteasome pathway has also been described as a mechanism to regulate transcriptional activity (*9*−*14*). For example, the proteolysis of the estrogen receptor α and its coactivator by the 26S proteasome is required for an efficient transactivation of target genes (*15*), while proteasome-mediated degradation of the p300 coactivator attenuates glucocorticoid signaling (*9*).

*G*lycogen *s*ynthase *k*inase 3β (GSK3β)[1] is an ubiquitously expressed serine/threonine kinase that phosphorylates a number of transcription factors (*16*). It also directly phosphorylates β-catenin, an Armadillo repeat protein family member involved in the Wnt-signaling cascade in vertebrates. In cell adhesion, β-catenin is present in cell−cell contacts thanks to a rapid turnover of the protein dependent on the axin/GSK3β/APC (*a*denomatous *p*olyposis *c*oli) complex (*17*). In the absence of Wnt signals, GSK3β phosphorylates β-catenin and induces its ubiquitination and degradation by the proteasome. Wnt signaling increases the amount of β-catenin by inactivating the GSK3β activity (*18*). This results in the stabilization and accumulation of β-catenin in the cytosol (*19*). Stable β-catenin can then bind to transcription factors of the lymphoid enhancer factor-1/*T* cell factor (LEF-1/TCF) family and is transported to the nucleus, resulting in changes in gene expression (*20*). In the nucleus,

† This work was supported by Grant No. 8640 from the Shriners of North America.

* To whom correspondence should be addressed. Genetics Unit, Shriners Hospital for Children, 1529 Cedar Avenue, Montréal (Québec), Canada, H3G 1A6. Tel.: 514-282-7155. Fax: 514-842-5581. E-mail: rst-arnaud@shriners.mcgill.ca.

‡ Shriners Hospital for Children.

§ McGill University.

[1] Abbreviations: αNAC: *N*ascent polypeptide associated complex *A*nd *C*oactivator alpha; GSK3β: glycogen synthase kinase 3β; DN-GSK3β: dominant negative mutant of glycogen synthase kinase 3β; AP-1: activating protein-1; JNK: c-Jun amino-terminal kinase; DMEM: Dulbecco's modified eagle medium; indirubin: 5-iodo-indirubin-3′-monoxime; EDTA: (ethylenedinitrilo) tetraacetic acid; EGTA: ethylene glycol-bis(β-aminoethyl ether)-*N*,*N*,*N*′,*N*′-tetraacetic acid; PMSF: phenylmethylsulfonyl fluoride; GST: glutathione-*S*-transferase; SDS: sodium dodecyl sulfate; DTT: dithiothreitol; SDS−PAGE: SDS−polyacrylamide gel electrophoresis DAB: 3,3′-diaminobenzidine; DAPI: 4′,6-diamidino-2-phenylindole; PVDF: poly(vinylidene difluoride); HRP: horseradish peroxidase; mmp-9: matrix metalloproteinase-9.

10.1021/bi036256+ CCC: $27.50
Published on Web 02/19/2004

β-catenin thus functions as a coactivator of LEF-1/TCF-dependent transcription.

The AP-1 family member c-Jun is degraded by the ubiquitin pathway (*21*, *22*). The amino-terminal region of c-Jun binds the c-Jun amino-terminal kinase (JNK), a member of the stress activated protein kinases (*23*). JNK targets nonphosphorylated c-Jun for ubiquitination and degradation in normally growing cells (*21*, *24*). Following JNK activation by various stimuli, phosphorylation of c-Jun protects it from ubiquitination and prolongs its half-life (*7*, *25*). JNK phosphorylates c-Jun at positions Ser63 and Ser73 within the c-Jun transcriptional activation domain, an essential step for the activating function of c-Jun (*26*). Interestingly, ubiquitination-independent c-Jun degradation by the proteasome has also been observed (*27*).

It has been demonstrated that GSK3β can phosphorylate c-Jun at C-terminal sites, resulting in the inhibition of the DNA-binding activity of c-Jun (*28*). In resting cells, in which AP-1 activity is low, c-Jun is phosphorylated on three amino acid residues located near the C-terminal DNA-binding domain (*29*). Activation of resting cells results in specific dephosphorylation of the C-terminal domain of c-Jun and leads to increased AP-1 DNA binding (*29*). It is likely that cell stimulation activates the N-terminal domain of c-Jun in parallel with inhibition of GSK3β activity to prevent phosphorylation of the c-Jun C-terminus, resulting in increased DNA-bound AP-1 complexes and enhanced AP-1 activity.

The *n*ascent polypeptide-associated complex *a*nd *c*oactivator alpha (αNAC) was first described to be involved in some aspects of translational control (*30*), but subsequently was also shown to function as a transcriptional coactivator by potentiating the activity of the chimeric Gal4-VP16 activator (*31*) and of c-Jun homodimers (*32*, *33*).

The degradation of αNAC may have profound consequences for its subcellular localization and its coactivation function. We present results demonstrating that αNAC is regulated by the proteasome pathway. We showed that its degradation was dependent upon its phosphorylation by GSK3β. The stabilization of αNAC, by inhibition of the GSK3β signal, or of the proteasome activity, induced the nuclear accumulation of the protein. Increases in the amount of nuclear αNAC potentiated its coactivating function.

MATERIALS AND METHODS

Cell Culture. COS-7 African green monkey kidney cells were maintained in low glucose DMEM supplemented with 10% fetal bovine serum at 37°C in 5% CO_2. All transient transfections were performed using the GenePorter transfection reagent (5 μL/μg DNA) according to the manufacturer's procedure (Gene Therapy System, San Diego, CA).

Constructs (subcloning details and vector maps available on request). The Flag epitope was inserted into the pSI mammalian expression vector (Promega, Madison, WI) to give the pSI-Flag plasmid. The cDNAs for the C-terminal deletion mutant Δ151−215 and single point mutants T157A, T159A, T161A, and S166A were obtained by PCR cloning (primer sequences available on request). The cDNAs encoding wild-type αNAC or mutants were inserted in-frame into pSI-Flag to yield the pSI-NAC-Flag expression vectors.

Pulse−Chase. The COS-7 cells were plated at 3.2×10^5 cells/60-mm plate 24 h prior to transfection, and transiently transfected with 3 μg of pSI-NAC-Flag or mutant, and 3 μg of pBlueScript (Stratagene, La Jolla, CA). At 48 h post-transfection, the cells were incubated for 1 h in methionine- and cysteine-free DMEM (ICN, Irvine, CA), and then labeled for 30 min with 100 μCi/mL of [^{35}S]methionine (ICN). The cells were washed and chased in complete medium supplemented with 1 mM excess of nonradioactive methionine for 30 min to 8 h before harvest. The proteasome inhibitor lactacystin (10 μM; Peptide Institute, Louisville, KY) (*34*), the thiol protease inhibitor E-64-d (25 μM; Peptide Institute), and the GSK3β inhibitor 5-iodo-indirubin-3′-monoxime (indirubin) (*35*) (20 μM, Calbiochem, La Jolla, CA) were added with the first incubation in methionine- and cysteine-free medium and during the pulse and the chase as well. The cells were washed and lysed in 2× lysis buffer (100 mM Tris-Cl pH 7.4, 300 mM NaCl, 2 mM EDTA, 2 mM EGTA, 2% Triton X-100) in the presence of 5 μg/mL antiproteases (leupeptin, aprotinin, and pepstatin A) and 1 mM PMSF. The lysates were diluted with H_2O to reach 1× lysis buffer. The cell extracts were incubated overnight at 4 °C with 40 μL of EZview Red anti-Flag M2 affinity gel (Sigma, Saint-Louis, MO), or with 20 μL of anti-GST affinity gel as a negative control (Santa Cruz Biotechnology Inc., Santa Cruz, CA). The affinity gel-purified proteins were extensively washed in 1× lysis buffer, resuspended in SDS sample buffer without DTT, and resolved by a 12% SDS−PAGE. The intensity of the signals was quantified using a Typhoon 8600 PhosphorImager (Amersham-Pharmacia Canada, Baie d'Urfé, QC).

Immunocytochemistry. COS-7 cells were plated at 1.2×10^5 cells/35-mm plate, on gelatin-coated cover slips. Twenty-four hours later, the cells were transiently transfected with 0.4 μg of pSI-NAC-Flag and 1.6 μg of pBlueScript (Stratagene). At 24 h post-transfection, the cells were treated for 4 h with the proteasome inhibitors lactacystin (25 μM) (*34*), MG-132 (20 μM, Calbiochem) (*36*), and epoxomicin (20 μM, Calbiochem) (*37*), or E-64-d (25 μM), indirubin (10, 20, and 50 μM), or vehicle. After treatment, the cells were fixed in 4% paraformaldehyde, permeabilized with 0.2% Triton X-100, and the quenching of endogenous peroxidase activity was performed with 1% H_2O_2. Following blocking with 1% Blocking Reagent (Roche Molecular Diagnostics, Laval, QC) supplemented with 0.2% Tween-20, the cells were incubated with the anti-Flag M2 antibody (Sigma), then incubated with the secondary biotinylated anti-mouse IgG antibody (Vector Laboratories Inc., Burlingame, CA). After washes, the cells were incubated in the Avidin Biotin peroxidase reagent (Vector Lab. Inc.). The peroxidase staining was resolved with DAB reagent. For the results presented in Figure 6, HeLa cells were transfected with 2 μg of pcDNA3-R85, an expression vector for a myc-tagged dominant-negative (DN) GSK3β mutant (*38*). Cells were fixed and treated as described above, and then incubated with a polyclonal anti-αNAC antibody (1:50 dilution) (*39*) and a monoclonal anti-myc tag antibody (1:200 dilution) (Santa Cruz Biotechnology). The cells were then incubated for 1−2 h at room temperature with a fluorescein isothiocyanate-conjugated anti-mouse IgG secondary antibody (dilution 1:500) to reveal the myc-tagged DN-GSK3β and a rhodamine-conjugated anti-rabbit IgG secondary antibody (dilution 1:500) to detect endogenous αNAC protein. Coverslips were mounted in Vectashield (with DAPI) mounting medium (Vector Labo-

ratories). All results were visualized on a Leica DM-R microscope at 200×.

In Vivo Phosphorylation Assays. At 48 h post-transfection, the pSI-NAC-Flag transfected COS-7 cells were treated for 1 h with lactacystin (10 μM), E-64-d (25 μM), indirubin (20 μM), or the corresponding vehicle, followed by permeabilization with 0.6 U/mL Streptolysin O (Sigma) and labeling for 1 h with 50 μCi of [γ-^{32}P]ATP (Amersham-Pharmacia), as described by Carter (*40*), in the presence of inhibitors where indicated in figure legends. The cells were lysed in 2× lysis buffer in the presence of inhibitors of phosphatases (2 mM β-glycerophosphate, 2 mM orthovanadate, 5 mM sodium pyrophosphate), and of proteases (5 μg/mL leupeptin, aprotinin, pepstatin A, and 1 mM PMSF). The cell lysates were diluted with H_2O to reach 1× lysis buffer. The radiolabeled cell extracts were incubated overnight at 4°C with anti-Flag M2 affinity gel (Sigma). The affinity gels were extensively washed in 1× lysis buffer and resuspended in SDS sample buffer in absence of DTT. Immunoprecipitates were run on 12% SDS−PAGE. The gel was subsequently dried and exposed at −80°C. The intensity of the signals was quantified using the Typhoon PhosphorImager. To control for protein expression levels, one-third of the lysates were run onto a 12% SDS−PAGE and transferred to a PVDF membrane. The membrane was blocked and incubated with the anti-NAC antibody. After washes, the membrane was incubated with the anti-rabbit secondary antibody conjugated to HRP (Amersham-Pharmacia). The signal was revealed with the ECL+Plus kit (Amersham-Pharmacia) and quantified with the Typhoon PhosphorImager.

In Vitro Kinase Assays. Full-length αNAC, deletion and point mutant cDNAs were subcloned in-frame at their C-termini with the Intein-Chitin binding domain of the $pTYB_2$ expression vector (New England Biolabs Ltd., Mississauga, ON). The recombinant proteins were produced and purified following the manufacturer's procedure (NEB). For in vitro kinase assays, 2 μg of the recombinant proteins were incubated for 30 min at 30°C in GSK3β buffer (20 mM Tris-Cl pH 7.5, 10 mM $MgCl_2$, 5 mM DTT) with 2.5 units of GSK3β (Sigma) and 5 μCi of [γ-^{32}P]ATP, and then resolved by a 12% SDS−PAGE.

Luciferase Assays. COS-7 cells were seeded at 1.2×10^5 cells/well in 6-well plates and transiently transfected the following day using 6 μL/well of the Lipofectamine reagent (Invitrogen Canada Inc., Burlington, ON). Transfections used 300 ng of expression vectors for wild-type αNAC or the T159A point mutant, and 300 ng of the pCI-c-Jun expression plasmid (*32*). The reporter vector (100 ng) was mmp-9 pGL3, which contains the proximal 670 bp of the mmp-9 gene promoter driving luciferase (*41*). Variations in transfection efficiency were monitored with 40 ng of the pSV_6tkCAT reporter (*42*). The total amount of DNA was completed at 2 μg using the inert pBlueScript plasmid (Stratagene). Cells were maintained in 0.5% serum throughout and lysates were prepared in the reporter gene assay lysis buffer (Roche Molecular Biochemicals, Laval, QC) 48 h post-transfection. One hundred microliters of cell lysate were used for single luciferase reporter assays following the manufacturer's instructions (Promega). Luciferase activity was measured with a Monolight 2010 luminometer (Analytical Luminescence Laboratory, San Diego, CA). Relative light units were normalized to CAT expression assayed by the CAT Elisa system (Roche Diagnostics, Indianapolis, IN). The expression level detected in cells transfected with the mmp-9 pGL3 reporter alone was arbitrarily ascribed a value of 1. The expression level of transfected proteins was controlled by immunoblotting with appropriate antibodies (data not shown).

RESULTS

Proteasome Inhibitor Lactacystin Increases the Metabolic Stability of αNAC. It is well established that inhibition of the 26S proteasome by lactacystin leads to a stabilization and accumulation of proteins that are usually metabolized by this pathway (*43*). To determine whether αNAC was degraded by the 26S proteasome, we employed COS-7 cells, which express detectable levels of endogenous αNAC (not shown), and transfected them with the αNAC-Flag expression vector. The transfected cells were pulse-labeled with [^{35}S]methionine for 30 min and chased for increasing periods of time. Immunoprecipitation showed that the level of radiolabeled αNAC-Flag decreased significantly slower in lactacystin-treated cells (Figure 1C) than in control cells (Figure 1A), whereas the thiol protease inhibitor E-64-d (Figure 1B) had no effect on the degradation of αNAC in COS-7 cells. In these experiments, the αNAC-Flag proteins could be resolved as a doublet reflecting differentially phosphorylated forms of the protein (ref *33* and Quélo and St-Arnaud, unpublished observations). Pulse-labeled αNAC-Flag protein levels decreased gradually with a calculated half-life of 1.8 h, in contrast to protein from the lactacystin-treated cells that exhibited a longer half-life (>8 h) (Figure 1D). These results strongly suggest that αNAC undergoes proteasome-mediated proteolysis.

Inhibition of the Proteasome Activity Induces the Nuclear Translocation of αNAC. The inactivation of the proteasome-dependent degradation pathway results in the accumulation of some proteins, such as β-catenin (*44*), and their translocation to the nucleus. To determine the localization of αNAC after inhibition of the proteasome, the transfected COS-7 cells were treated with the proteasome inhibitors lactacystin (*34*), MG-132 (*36*), or epoxomicin (*37*), or the thiol protease inhibitor E-64-d for 4 h, and immunostained with the anti-Flag M2 antibody (Figure 2). Immunodetection of steady-state expression patterns revealed that αNAC-Flag had a cytoplasmic and perinuclear expression pattern (panel b), identical to endogenous αNAC (see Figure 6, bottom panel). Some nuclear staining could also be detected under steady-state conditions (Figure 2b). αNAC translocated to the nucleus after inhibition of the 26S proteasome activity by treatment of cells with lactacystin (panel c), MG-132 (panel e), or epoxomicin (panel f). This translocation was specific to the inhibition of the proteasome since no effect was observed after treatment with E-64-d (panel d). Thus, the inhibition of the rapid turnover of αNAC led to its stabilization and accumulation in cells. This resulted in its nuclear translocation, where the protein may exert its coactivating function.

αNAC Is Phosphorylated by GSK3β in Vivo. Inhibition of the GSK3β kinase was shown to stabilize c-Jun (*8*) and β-catenin (*18*) in target cells. Mutations of the GSK3β phosphorylation sites within β-catenin leads to an accumulation of the mutant protein (*19*, *44*, *45*). These results stimulated experiments to test whether αNAC was a substrate

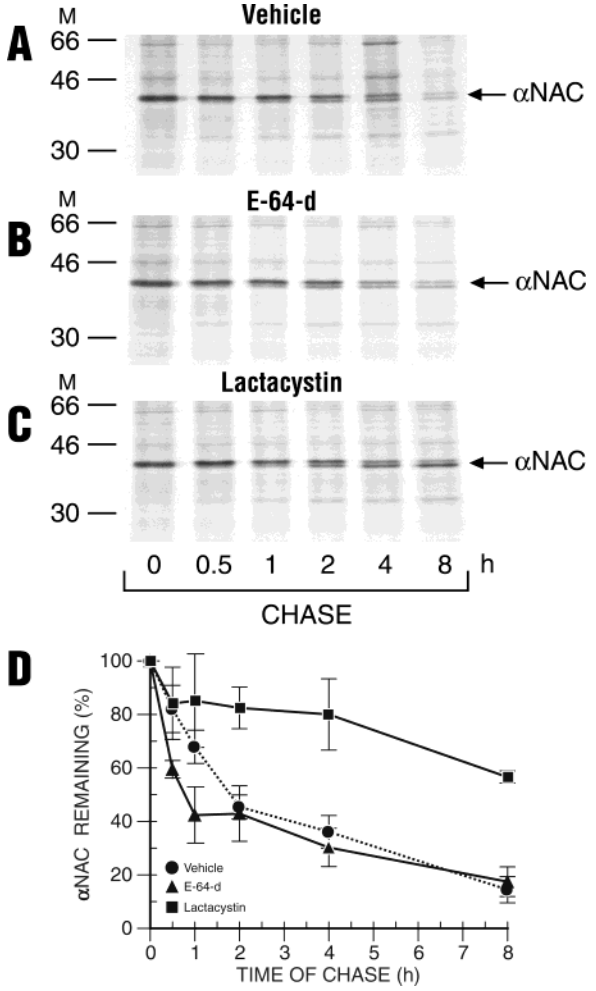

FIGURE 1: The 26S proteasome degrades αNAC. (A, B, C) Pulse-chase analysis. At 48 h post-transfection with an αNAC-Flag expression vector, COS-7 cells were pulse-labeled for 30 min with [^{35}S]-methionine and lysed at the indicated times. Lactacystin (panel C, 10 μM), E-64-d (panel B, 25 μM), or vehicle (panel A) were added during the pulse and the chase. Flag-tagged proteins were purified with anti-Flag M2 affinity resin and revealed by autoradiography. M, molecular size markers. (Panel D) quantification. The intensity of the signal from the blots shown in A−C were quantified using a PhosphorImager; the signal at time 0 of the chase was set as 100%. The graph shows mean ± SEM of three separate experiments. The half-life of αNAC was calculated at 1.8 h in untreated cells but increased to more than 8 h in response to lactacystin treatment.

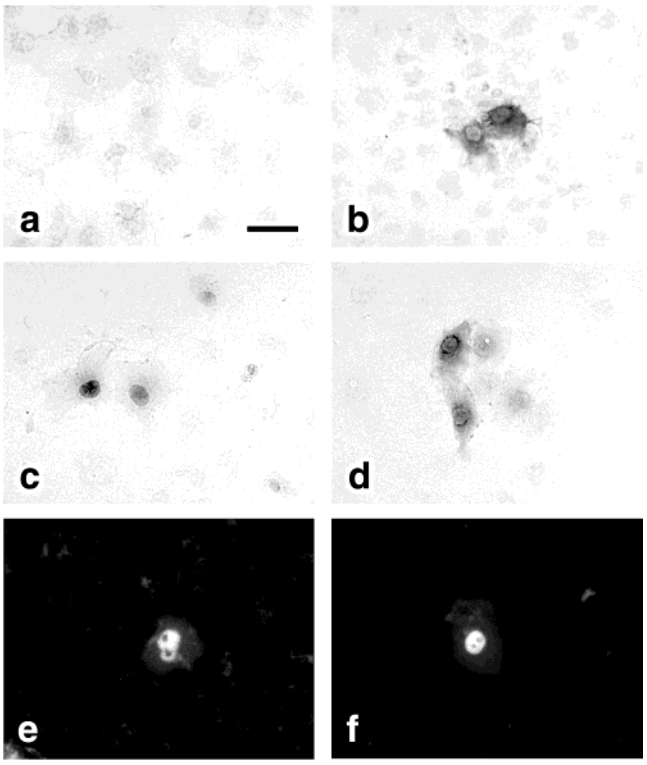

FIGURE 2: Localization of αNAC in cells treated with inhibitors of the proteasome. COS-7 cells were transiently transfected with the αNAC-Flag expression vector. At 24 h post-transfection, COS-7 cells were treated with lactacystin (c, 25 μM), E−64-d (d, 25 μM), MG-132 (e, 20 μM), epoxomicin (f, 20 μM), or vehicle (a, b). After 4 h of treatment, the cells were immunostained with the anti-Flag M2 antibody (b−f). Detection was by peroxidase staining (a−d) or indirect fluorescence (e, f). Background staining was assessed by staining cells transfected with the empty expression vector (panel a). Bar = 100 μm.

of GSK3β in cells (Figure 3). Metabolic labeling of intact cells after permeabilization (*40*) showed that the αNAC-Flag protein was phosphorylated in vivo (upper panel, lane 2). Inhibition of the endogenous GSK3β activity by indirubin (*35*) reduced the phospholabeling of αNAC and thus confirmed that αNAC was a substrate of GSK3β in vivo (lane 3). Normalization of the phosphorylation signal to protein expression levels (Figure 3, lower panel) using the Scion Image software (Scion Corporation, Md) confirmed that indirubin treatment reduced phosphorylation levels by 25%.

Inhibition of GSK3β Blocks αNAC Degradation. We next investigated the impact of phosphorylation by GSK3β on the stability of αNAC. For that purpose, pulse-chase analyses were performed with the wild-type αNAC in the presence of indirubin or vehicle. Following immunoprecipitation, the level of pulse-labeled αNAC-Flag proteins decreased slower in indirubin-treated cells (Figure 4A, lower panel) than in vehicle-treated cells (Figure 4A, upper panel). The half-life of the protein increased by 2.5-fold after indirubin treatment and was measured at 4.5 h (Figure 4B). These results strongly suggest that the inhibition of the GSK3β activity prevented αNAC degradation by the 26S proteasome and led to an accumulation of the protein in cells.

Inhibition of the GSK3β Activity Leads to the Nuclear Translocation of αNAC. We examined the subcellular localization of αNAC in COS-7 cells when GSK3β activity was inhibited by treatment with indirubin or by overexpression of a dominant-negative GSK3β (DN-GSK3β) mutant. We performed immunocytochemistry in COS-7 cells transiently transfected with expression vectors for αNAC and the subcellular localization of the Flag-tagged proteins was observed with the anti-Flag M2 antibody. As previously observed, the immunostaining revealed a predominant perinuclear and cytoplasmic distribution of αNAC (Figure 5a; see also Figure 6, lower panel). In contrast, the protein located to the nucleus of cells after inhibition of the GSK3β activity by treatment with indirubin. The indirubin effect was dose-dependent (Figure 5, panels b, c, and d), with the higher nuclear staining observed at 50 μM. Cells were also transfected with a dominant negative mutant form of GSK3β (*38*). Figure 6 shows a field of four cells (top panel, DAPI staining) that expressed endogenous αNAC (bottom panel). One of these cells also expressed the DN-GSK3β mutant (middle panel). The endogenous αNAC protein localized to

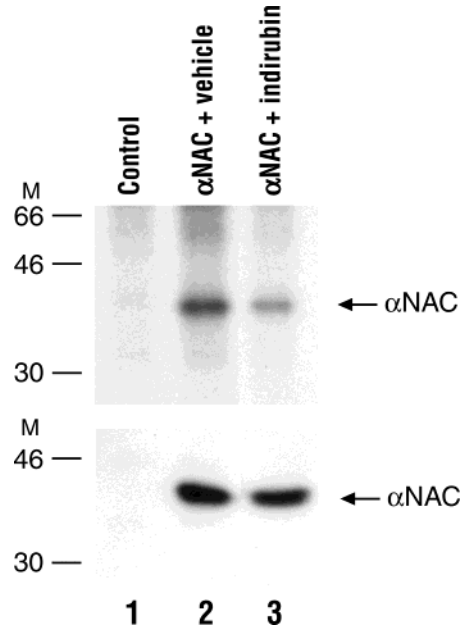

FIGURE 3: GSK3β phosphorylates αNAC in vivo. COS-7 cells were transfected with the αNAC-Flag expression vector, and treated for 2 h with the GSK3β inhibitor, indirubin (20 μM), or vehicle. After labeling with [γ-^{32}P]ATP, the Flag-tagged proteins were immunoprecipitated. The phosphorylated proteins were revealed by autoradiography (upper panel) and the expression of αNAC by immunoblotting with the anti-NAC antibody (lower panel). M, molecular size markers.

the cytoplasm, except in the cell that coexpressed the DN-GSK3β protein, where it also accumulated in the nucleus (Figure 6, bottom panel). Taken together, these results show that inhibition of GSK3β activity, either with chemical inhibitors or dominant negative mutants, promoted nuclear localization of αNAC.

Identification of the GSK3β Phosphoacceptor Site. To identify the GSK3β phosphoacceptor site within αNAC, wild-type αNAC, deletion and point mutants were produced and purified in *Escherichia coli* using pTYB$_2$-based expression vectors, which yield recombinant proteins devoid of an associated fusion moiety. These were used for in vitro kinase assays with recombinant GSK3β (Figure 7). The maltose binding protein (MaBP), produced in a similar fashion, was used as a negative control, whereas the recombinant protein myelin basic protein (MyBP) served as positive control for the GSK3β activity. In vitro kinase assays demonstrated that αNAC was a substrate of GSK3β in vitro (Figure 7A, upper panel, lane 4). In these assays, a minor phosphorylated product with faster electrophoretic mobility was observed. This band may represent a degradation product or a differentially posttranslationally modified recombinant αNAC molecule. Deleting residues 151−215 from the recombinant αNAC completely inhibited GSK3β phosphorylation of the protein (Figure 7A, upper panel, lane 5), suggesting that the GSK3β phosphoacceptor site resides in the carboxy-terminal end of αNAC. The decrease observed with the Δ151−215 mutant was not due to a lower amount of the recombinant protein, as shown by Gel Code Blue staining (Figure 7A, lower panel).

We then identified the phosphoacceptor site by using point mutants of the serine and threonine residues in the C-terminal region of αNAC. The residue threonine 159 was identified

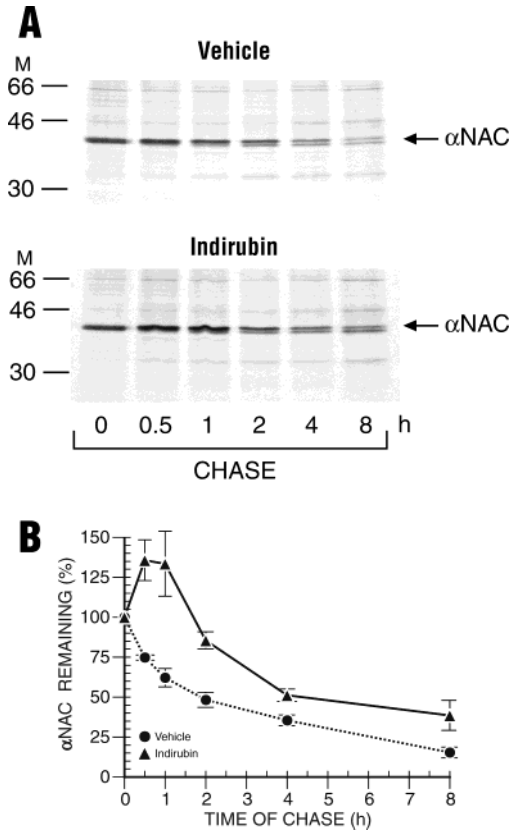

FIGURE 4: Proteasome degradation of αNAC depends on GSK3β phosphorylation. (A) Pulse-chase analysis. After transfection with the αNAC-Flag expression vector, the ^{35}S-labeled COS7 cells were chased for the times indicated, in the presence of indirubin (lower panel, 20 μM) or vehicle (upper panel). The Flag-tagged proteins were purified with anti-Flag M2 affinity gel and revealed by autoradiography. M, molecular size markers. (B) Quantification. The half-life of αNAC was calculated at 1.8 h in vehicle-treated cells, but increased 2.5-fold in response to indirubin treatment (4.5 h).

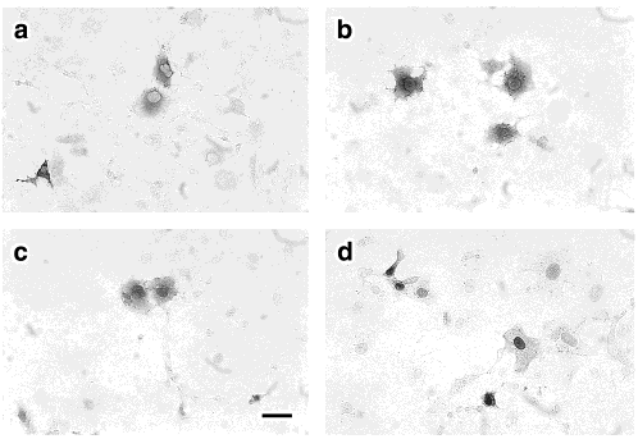

FIGURE 5: Nuclear translocation of αNAC following inhibition of GSK3β activity. COS-7 cells were transiently transfected with the αNAC-Flag expression vector. At 24 h post-transfection, the cells were treated for 4 h with increasing concentration of indirubin (b, c, d) or vehicle (a). The peroxidase staining was revealed with anti-Flag M2 antibody. (a) vehicle; (b) 10 μM indirubin, (c) 20 μM indirubin; (d) 50 μM indirubin. Bar = 50 μm.

as the GSK3β phosphoacceptor site in vitro (Figure 7B, upper panel, lane 4). Staining of the proteins demonstrated that the decreased signal obtained with the T159A mutant was not due to a reduced amount of protein (Figure 7B, lower panel).

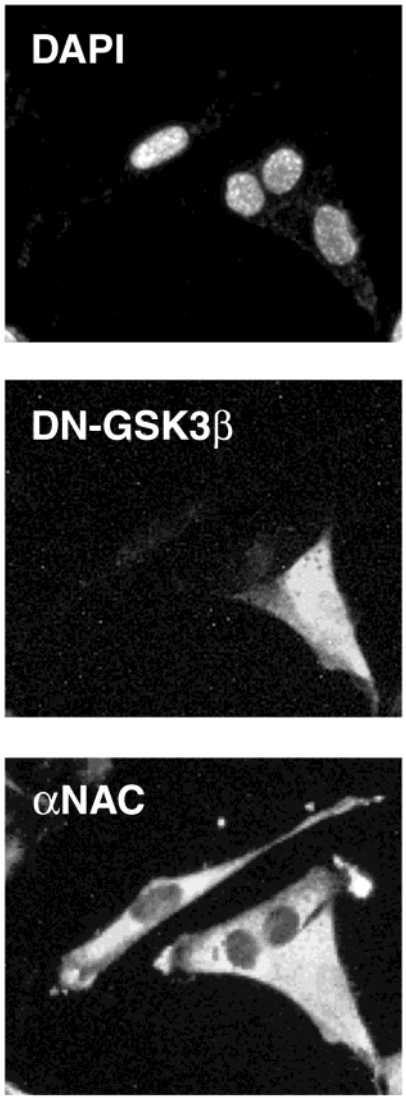

FIGURE 6: Nuclear accumulation of αNAC in cells expressing a dominant-negative GSK3β mutant. HeLa cells were transiently transfected with pcDNA3-R85, an expression vector for a myc-tagged dominant-negative (DN) GSK3β mutant. Indirect immunofluorescence with an anti-myc epitope and anti-αNAC antibodies revealed expression of the transfected DN-GSK3β mutant (middle panel) or the endogenous αNAC protein (bottom panel). DAPI stain in the mounting medium labeled the nuclei of all cells in the field (top panel). Note that endogenous αNAC was cytoplasmic in untransfected cells, but accumulated in the nucleus of cells expressing DN-GSK3β.

T159 Phosphoacceptor Site Is Functional in Cells. We transfected deletion and point mutants of αNAC-Flag in COS-7 cells and performed metabolic labeling with [γ-^{32}P]-ATP. Immunoprecipitated Flag-tagged proteins revealed a decrease in phosphorylation after deletion or mutation of the C-terminal region of αNAC (Figure 8A). The phosphorylation levels were measured by PhosphorImager, and controlled for protein expression levels (data not shown). The Δ151−215 mutant retained only 31% of the αNAC phosphorylation level, whereas the T159A point mutant lost 16% of the phosphorylation signal intensity (Figure 8B). It should be noted that mutation of the T159 phosphoacceptor residue and inhibition of GSK3β by treatment of cells with indirubin had identical effects on αNAC phosphorylation (Figure 8B). The very low phosphorylation level observed with the deleted

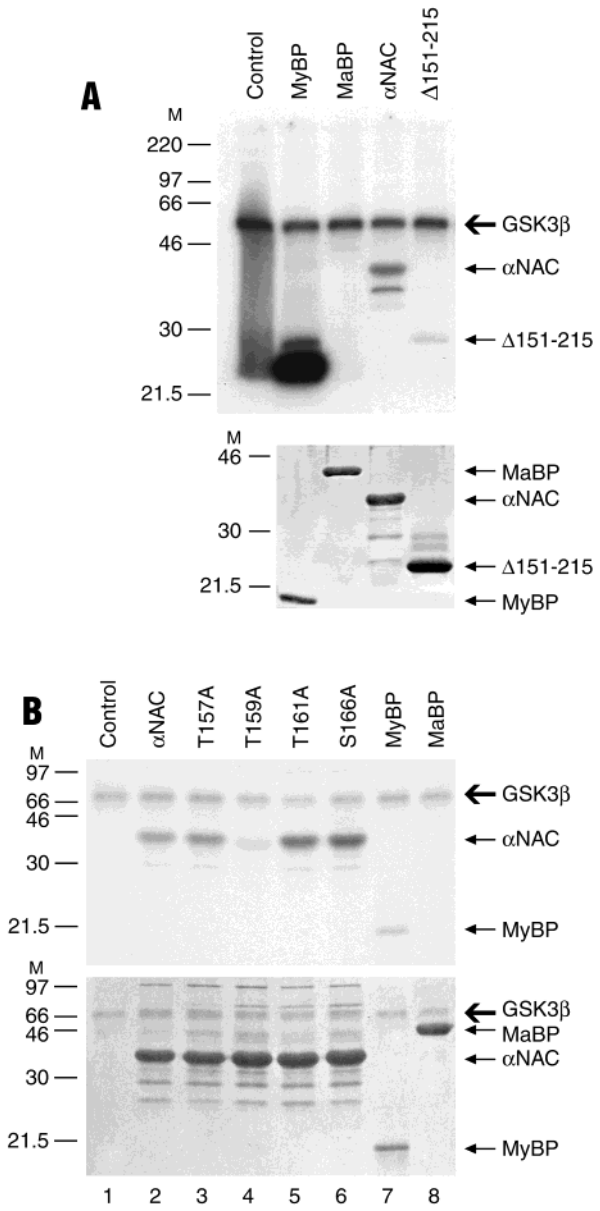

FIGURE 7: Identification of the GSK3β phosphoacceptor site. (A) Recombinant GSK3β was incubated with recombinant αNAC WT, or Δ151−215 deletion mutant, positive control (MyBP) or negative control (MaBP), in the presence of [γ-^{32}P]ATP. The ^{32}P-phosphorylated substrates were detected by autoradiography (upper gel). The lower gel shows Gel Code blue staining. The autophosphorylation of GSK3β was detected in this in vitro kinase assay (bold arrow). A significant decrease in GSK3β-dependent phosphorylation was observed with the Δ151−215 mutant. (B) In vitro GSK3β kinase assay was performed with single point mutants of αNAC C-terminal region (upper gel). A significant decrease in the phosphorylation level was observed with the T159A mutant (lane 4). The lower gel shows Gel Code blue staining. M, molecular size markers.

mutant was most likely due to the presence of other phosphoacceptor sites within the deleted C-terminal region.

As inhibition of GSK3β activity resulted in the relocalization of αNAC to the nucleus, we next examined the effect of mutating the GSK3β phosphoacceptor site on the coactivating function of αNAC. We performed transfections in COS-7 cells with expression vectors for wild-type or T159A αNAC proteins, c-Jun, and a luciferase reporter gene under the control of the mmp-9 gene promoter (*41*). Under the conditions selected, c-Jun modestly stimulated the expression

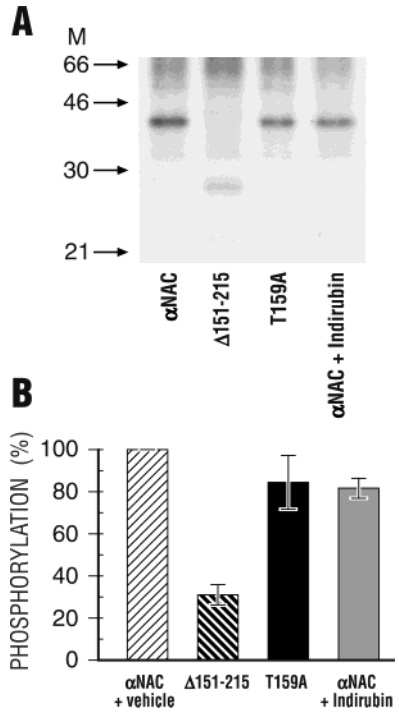

FIGURE 8: The T159 phosphoacceptor site is functional in cells. COS-7 cells were transfected with wild-type αNAC, with or without indirubin treatment, the Δ151−215 deletion mutant, or the T159A point mutant expression vectors, and radiolabeled with [γ-^{32}P]ATP following permeabilization. (A) After immunoprecipitation with the anti-Flag M2 beads, the phosphorylation status of the Flag-tagged proteins was revealed by autoradiography (representative experiment). (B) The phosphorylation levels of wild-type αNAC and mutant proteins were calculated using a Typhoon PhosphorImager and controlled for protein expression levels. With the phosphorylation signal of wild-type αNAC arbitrarily set at 100%, phosphorylation of the other samples was calculated as Δ151−215: 31%; T159A: 84%; indirubin treatment: 82%.

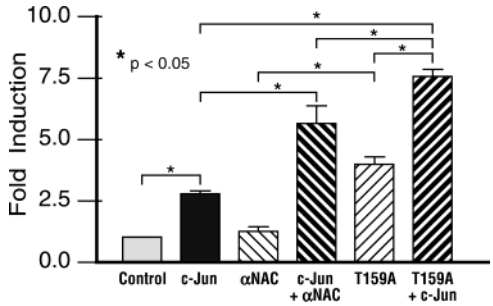

FIGURE 9: Effect of mutating the GSK3β phosphoacceptor site on αNAC-mediated coactivation of c-Jun-dependent transcription. COS-7 cells were transfected with expression vectors for c-Jun, wild-type αNAC, or the T159A mutant, alone or in combinations. The reporter construct contained the proximal 670 bp of the mmp-9 gene promoter driving luciferase. After 48 h in low serum, the cells were lysed and luciferase assays were performed. The expression level detected in cells transfected with the reporter construct alone was arbitrarily ascribed a value of 1. Results are mean ± SEM of three independent transfections.

of the reporter gene, while the wild-type αNAC protein was without effect (Figure 9). When coexpressed with c-Jun, αNAC potentiated AP-1-dependent transcription from the mmp-9 promoter (Figure 9). Interestingly, the T159A phosphoacceptor mutant, which accumulates in the nucleus (data not shown), led to increased transcription from the mmp-9 promoter, presumably through interaction with endogenous c-Jun proteins. When coexpressed with c-Jun, the T159A αNAC mutant strongly potentiated the transcriptional activity of c-Jun (Figure 9). The T159A coactivating activity was significantly higher than the activity measured for its wild-type counterpart (Figure 9). Thus, blocking the phosphorylation of αNAC by GSK3β leads to an increase in the transcriptional regulatory activity of αNAC.

DISCUSSION

The regulation of the expression and degradation of transcription factors and their coactivators are important for an efficient regulation of target gene transcription (*6*, *9*−*11*, *13*, *15*). c-Jun degradation, subcellular localization, and transcriptional activity is tightly regulated in cells (*7*, *29*, *46*, *47*). αNAC was previously demonstrated to be a transcriptional coactivator for c-Jun (*32*, *33*). In this study, we have addressed the control of αNAC protein levels and subcellular localization by inhibition of the proteasome pathway and suppression of GSK3β signaling.

Our results strongly suggest that posttranslational modifications of αNAC resulted in its regulated degradation by the 26S proteasome in vivo. The αNAC protein was a substrate for GSK3β-dependent phosphorylation in vivo and in vitro, and this posttranslational modification occurred on residue T159 of the molecule. Since the inhibition of the endogenous GSK3β activity blocked αNAC degradation, we conclude that GSK3β-dependent phosphorylation of αNAC is the key signal that directs the protein for proteolysis by the 26S proteasome. Inhibition of αNAC degradation by inhibition of the proteasome or GSK3β activities moreover resulted in the accumulation of αNAC in the nuclei of cells and increased αNAC coactivating potency.

Ubiquitination and proteasome-dependent degradation has been reported for transcriptional coactivators that modulate the activity of several classes of transcription factors, such as nuclear receptors (*9*, *12*, *15*), octamer proteins (*10*, *11*), cardiac MEF2 factors (*13*), and AP-1 family members (*14*, *48*). Thus, regulating the stability and level of transcriptional coactivators may appear as a general mechanism to modulate transcriptional activity. In some instances, ubiquitination of the coactivator molecule was unambiguously demonstrated (*14*). In other cases, ubiquitination was inferred based on interaction of the coactivator with a ubiquitin ligase protein and the effect of proteasome inhibitors (*11*, *13*). Our attempts to detect ubiquitinated αNAC species were not successful (not shown). While this may reflect the difficulty in isolating polyubiquitinated proteins upon inhibition of the proteasome (*49*), it is worth mentioning that ubiquitination-independent proteasomal degradation was recently demonstrated for AP-1 family members (*27*, *50*). It remains possible that αNAC, a coactivator of the c-Jun AP-1 dimer (*32*, *33*), is targeted to the proteasome via a similar ubiquitination-independent pathway.

It appeared that the intracellular pool of αNAC was recognized and phosphorylated by an active GSK3β in cells. Inhibition of endogenous GSK3β activity by indirubin treatment or through a dominant-negative GSK3β mutant led to nuclear accumulation of αNAC. Permeabilization and phosphorylation studies revealed that the T159 phosphoacceptor site was functional in cells. Labeling of phosphoproteins in permeabilized, intact cells is a powerful experimental approach to study protein kinase-catalyzed phosphoryla-

tion reactions and identify relevant substrates (*40*). We treated cells with the inhibitor indirubin to confirm that αNAC was a substrate of GSK3β in vivo. Indirubin was also shown to inhibit several cyclin-dependent kinases such as CDK1 (*35*). However, indirubin inhibits GSK3β more potently than it does CDK1 (*35*). Moreover, no consensus site for phosphorylation by CDKs was identified within the αNAC amino acid sequence using NetPhos, the prediction server of the Center for Biological Sequence Analysis of the Technical University of Denmark. This supports the hypothesis that αNAC is a bona fide GSK3β substrate in cells.

In the permeabilization experiments, the phospholabeling of the T159A mutant was only slightly reduced. This most likely results from the presence of several putative phosphoacceptor sites for various other protein kinases within the αNAC sequence (18 serine and 18 threonine residues). A similar reduction of phosphorylation was obtained after inhibition with indirubin, however, which confirmed that residue T159 was the only functional GSK3β phosphoacceptor site in cells. By contrast, an important decrease in phospholabeling was observed with the Δ151−215 mutant, presumably related to the presence of 10 putative phosphoacceptor sites in the deleted region.

Nuclear accumulation of αNAC was induced by inhibition of the GSK3β activity. Under steady-state conditions, a small portion of αNAC was localized to the nucleus of cells (Figure 2), suggesting that the protein may shuttle to and from the nucleus constitutively. Our results showing a nuclear staining of αNAC following proteasome inhibition or GSK3β inhibition suggest that the cellular accumulation of αNAC, achieved by influencing the regulated degradation of αNAC by the proteasome pathway, resulted in a higher nuclear entry of the molecule. A similar nuclear pattern was obtained with another GSK3β inhibitor, SB216763 (data not shown). We hypothesize that the translocation to the nucleus was mediated by an unidentified nuclear localization sequence, or in conjunction with a transcriptional partner, which leads to the availability of αNAC in the nucleus to exert its function as a transcriptional coactivator (*31*, *33*). By analogy to the β-catenin pathway, αNAC nuclear translocation may occur in a complex with transcription factors such as c-Jun, with which αNAC is known to interact (*33*). Full c-Jun transcriptional activity also requires dephosphorylation of GSK3β phosphoacceptor sites (*29*) and inhibition of proteasome degradation (*24*). It is tempting to speculate that some of the signals that control c-Jun phosphorylation by GSK3β and its stability will also impact on αNAC phosphorylation and half-life. Affecting both the stability of αNAC and its partner c-Jun, through signaling or treatment with GSK3β or proteasome inhibitors as described herein, would result in cellular accumulation of the proteins, their translocation to the nucleus and their saturation effects on transcription.

Indeed, we demonstrated that mutation of the GSK3β phosphoacceptor site resulted in a significant increase in αNAC coactivating function. The transcription data presented in Figure 9 is the first demonstration of the AP-1-dependent coactivating function of αNAC on a natural transcriptional regulatory sequence, the mmp-9 gene promoter. Inhibition of the endogenous GSK3β activity by treatment of cells with low doses of indirubin or the SB216763 inhibitor also resulted in a slight increase in αNAC-mediated coactivation (data not shown). Overall, our results are consistent with a role for GSK3β phosphorylation in the control of the subcellular localization of αNAC with an impact on its coactivating function.

Since the degradation of αNAC by the proteasome appears to be a steady-state event, it will be of interest to determine the nature of putative inhibitory stimuli for αNAC degradation. In our present model, the phosphorylation of αNAC by GSK3β in the absence of signals would represent the initial event for the degradation of αNAC. The inactivation of GSK3β in response to an unknown upstream signal would then result in a hypophosphorylated αNAC that would become unavailable for the proteasome degradation machinery, would translocate to the nucleus, and potentiate transcription.

ACKNOWLEDGMENT

Dr. Shoukat Dedhar (University of British Columbia, Vancouver, BC) kindly provided the mmp-9 pGL3 plasmid, while the pcDNA3-R85 vector was a generous gift of Dr. Isabel Dominguez (Boston University School of Medicine). We used the PhosphorImager from the Centre for Bone and Periodontal Research of McGill University. We thank Mark Lepik for preparing the figures.

REFERENCES

1. Pillay, C. S., Elliott, E., and Dennison, C. (2002) Endolysosomal proteolysis and its regulation. *Biochem. J. 363*, 417−429.
2. Voges, D., Zwickl, P. and Baumeister, W. (1999) The 26S proteasome: a molecular machine designed for controlled proteolysis. *Annu. Rev. Biochem. 68*, 1015−1068.
3. Gorbea, C., Taillandier, D., and Rechsteiner, M. (1999) Assembly of the regulatory complex of the 26S proteasome. *Mol. Biol. Rep. 26*, 15−19.
4. Bochtler, M., Ditzel, L., Groll, M., Hartmann, C., and Huber, R. (1999) The proteasome. *Annu. Rev. Biophys. Biomol. Struct. 28*, 295−317.
5. Arrigo, A. P., Tanaka, K., Goldberg, A. L., and Welch, W. J. (1988) Identity of the 19S 'prosome' particle with the large multifunctional protease complex of mammalian cells (the proteasome). *Nature 331*, 192−194.
6. Conaway, R. C., Brower, C. S., and Conaway, J. W. (2002) Emerging roles of ubiquitin in transcription regulation. *Science 296*, 1254−1258.
7. Salvat, C., Jariel-Encontre, I., Acquaviva, C., Omura, S., and Piechaczyk, M. (1998) Differential directing of c-Fos and c-Jun proteins to the proteasome in serum-stimulated mouse embryo fibroblasts. *Oncogene 17*, 327−337.
8. Treier, M., Staszewski, L. M., and Bohmann, D. (1994) Ubiquitin-dependent c-Jun degradation in vivo is mediated by the delta domain. *Cell 78*, 787−798.
9. Li, Q., Su, A., Chen, J., Lefebvre, Y. A., and Hache, R. J. (2002) Attenuation of glucocorticoid signaling through targeted degradation of p300 via the 26S proteasome pathway. *Mol. Endocrinol. 16*, 2819−2827.
10. Boehm, J., He, Y., Greiner, A., Staudt, L., and Wirth, T. (2001) Regulation of BOB.1/OBF.1 stability by SIAH. *EMBO J. 20*, 4153−4162.
11. Tiedt, R., Bartholdy, B. A., Matthias, G., Newell, J. W., and Matthias, P. (2001) The RING finger protein Siah-1 regulates the level of the transcriptional coactivator OBF-1. *EMBO J. 20*, 4143−4152.
12. Baumann, C. T., Ma, H., Wolford, R., Reyes, J. C., Maruvada, P., Lim, C., Yen, P. M., Stallcup, M. R., and Hager, G. L. (2001) The glucocorticoid receptor interacting protein 1 (GRIP1) localizes in discrete nuclear foci that associate with ND10 bodies and are enriched in components of the 26S proteasome. *Mol. Endocrinol. 15*, 485−500.
13. Poizat, C., Sartorelli, V., Chung, G., Kloner, R. A., and Kedes, L. (2000) Proteasome-mediated degradation of the coactivator p300 impairs cardiac transcription. *Mol. Cell. Biol. 20*, 8643−8654.

14. Iwao, K., Kawasaki, H., Taira, K., and Yokoyama, K. K. (1999) Ubiquitination of the transcriptional coactivator p300 during retinoic acid induced differentiation. *Nucleic Acids Symp. Ser.* 207−208.
15. Lonard, D. M., Nawaz, Z., Smith, C. L., and O'Malley, B. W. (2000) The 26S proteasome is required for estrogen receptor-alpha and coactivator turnover and for efficient estrogen receptor-alpha transactivation. *Mol. Cell 5*, 939−948.
16. Frame, S., and Cohen, P. (2001) GSK3 takes centre stage more than 20 years after its discovery. *Biochem. J. 359*, 1−16.
17. Nakamura, T., Hamada, F., Ishidate, T., Anai, K., Kawahara, K., Toyoshima, K., and Akiyama, T. (1998) Axin, an inhibitor of the Wnt signaling pathway, interacts with beta-catenin, GSK-3beta and APC and reduces the beta-catenin level. *Genes Cells 3*, 395−403.
18. Aberle, H., Bauer, A., Stappert, J., Kispert, A., and Kemler, R. (1997) beta-catenin is a target for the ubiquitin-proteasome pathway. *EMBO J. 16*, 3797−3804.
19. Kikuchi, A. (1999) Roles of Axin in the Wnt signalling pathway. *Cell Signaling 11*, 777−788.
20. Hsu, S. C., Galceran, J., and Grosschedl, R. (1998) Modulation of transcriptional regulation by LEF-1 in response to Wnt-1 signaling and association with beta-catenin. *Mol. Cell. Biol. 18*, 4807−4818.
21. Fuchs, S. Y., Xie, B., Adler, V., Fried, V. A., Davis, R. J., and Ronai, Z. (1997) c-Jun NH2-terminal kinases target the ubiquitination of their associated transcription factors. *J. Biol. Chem. 272*, 32163−32168.
22. Hermida-Matsumoto, M. L., Chock, P. B., Curran, T., and Yang, D. C. (1996) Ubiquitinylation of transcription factors c-Jun and c-Fos using reconstituted ubiquitinylating enzymes. *J. Biol. Chem. 271*, 4930−4936.
23. Paul, A., Wilson, S., Belham, C. M., Robinson, C. J., Scott, P. H., Gould, G. W., and Plevin, R. (1997) Stress-activated protein kinases: activation, regulation and function. *Cell Signaling 9*, 403−410.
24. Fuchs, S. Y., Dolan, L., Davis, R. J., and Ronai, Z. (1996) Phosphorylation-dependent targeting of c-Jun ubiquitination by Jun N-kinase. *Oncogene 13*, 1531−1535.
25. Musti, A. M., Treier, M., and Bohmann, D. (1997) Reduced ubiquitin-dependent degradation of c-Jun after phosphorylation by MAP kinases. *Science 275*, 400−402.
26. Smeal, T., Binetruy, B., Mercola, D. A., Birrer, M., and Karin, M. (1991) Oncogenic and transcriptional cooperation with Ha-Ras requires phosphorylation of c-Jun on serines 63 and 73. *Nature 354*, 494−496.
27. Jariel-Encontre, I., Pariat, M., Martin, F., Carillo, S., Salvat, C., and Piechaczyk, M. (1995) Ubiquitinylation is not an absolute requirement for degradation of c-Jun protein by the 26 S proteasome. *J. Biol. Chem. 270*, 11623−11627.
28. de Groot, R. P., Auwerx, J., Bourouis, M., and Sassone-Corsi, P. (1993) Negative regulation of Jun/AP-1: conserved function of glycogen synthase kinase 3 and the Drosophila kinase shaggy. *Oncogene 8*, 841−847.
29. Boyle, W. J., Smeal, T., Defize, L. H., Angel, P., Woodgett, J. R., Karin, M., and Hunter, T. (1991) Activation of protein kinase C decreases phosphorylation of c-Jun at sites that negatively regulate its DNA-binding activity. *Cell 64*, 573−584.
30. Wiedmann, B., Sakai, H., Davis, T. A., and Wiedmann, M. (1994) A protein complex required for signal-sequence-specific sorting and translocation. *Nature 370*, 434−440.
31. Yotov, W. V., Moreau, A., and St-Arnaud, R. (1998) The alpha chain of the nascent polypeptide-associated complex functions as a transcriptional coactivator. *Mol. Cell. Biol. 18*, 1303−1311.
32. Quelo, I., Hurtubise, M., and St-Arnaud, R. (2002) alphaNAC requires an interaction with c-Jun to exert its transcriptional coactivation. *Gene Expr. 10*, 255−262.
33. Moreau, A., Yotov, W. V., Glorieux, F. H., and St-Arnaud, R. (1998) Bone-specific expression of the alpha chain of the nascent polypeptide- associated complex, a coactivator potentiating c-Jun-mediated transcription. *Mol. Cell. Biol. 18*, 1312−1321.
34. Fenteany, G., Standaert, R. F., Lane, W. S., Choi, S., Corey, E. J., and Schreiber, S. L. (1995) Inhibition of proteasome activities and subunit-specific amino-terminal threonine modification by lactacystin. *Science 268*, 726−731.
35. Leclerc, S., Garnier, M., Hoessel, R., Marko, D., Bibb, J. A., Snyder, G. L., Greengard, P., Biernat, J., Wu, Y. Z., Mandelkow, E. M., Eisenbrand, G. and Meijer, L. (2001) Indirubins inhibit glycogen synthase kinase-3 beta and CDK5/p25, two protein kinases involved in abnormal tau phosphorylation in Alzheimer's disease. A property common to most cyclin-dependent kinase inhibitors? *J. Biol. Chem. 276*, 251−260.
36. Lee, D. H., and Goldberg, A. L. (1996) Selective inhibitors of the proteasome-dependent and vacuolar pathways of protein degradation in *Saccharomyces cerevisiae*. *J. Biol. Chem. 271*, 27280−27284.
37. Meng, L., Mohan, R., Kwok, B. H., Elofsson, M., Sin, N., and Crews, C. M. (1999) Epoxomicin, a potent and selective proteasome inhibitor, exhibits in vivo antiinflammatory activity. *Proc. Natl. Acad. Sci. U.S.A. 96*, 10403−10408.
38. Dominguez, I., Itoh, K., and Sokol, S. Y. (1995) Role of glycogen synthase kinase 3 beta as a negative regulator of dorsoventral axis formation in Xenopus embryos. *Proc. Natl. Acad. Sci. U.S.A. 92*, 8498−8502.
39. Yotov, W. V., and St-Arnaud, R. (1996) Differential splicing-in of a proline-rich exon converts alphaNAC into a muscle-specific transcription factor. *Genes Dev. 10*, 1763−1772.
40. Carter, N. A. (1997) Permeabilization strategies to study protein phosphorylation. In Ausubel, F. M., Brent, R., Kingston, R. E., Moore, D. D., Seidman, J. G., Smith, J. A., and Struhl, K., Eds. *Current Protocols in Molecular Biology*, Vol. 4, pp 18.18.11−18.18.19, John Wiley and Sons, New York.
41. Gum, R., Lengyel, E., Juarez, J., Chen, J. H., Sato, H., Seiki, M., and Boyd, D. (1996) Stimulation of 92-kDa gelatinase B promoter activity by ras is mitogen-activated protein kinase kinase 1-independent and requires multiple transcription factor binding sites including closely spaced PEA3/ets and AP-1 sequences. *J. Biol. Chem. 271*, 10672−10680.
42. Courey, A. J., and Tjian, R. (1988) Analysis of Sp1 in vivo reveals multiple transcriptional domains, including a novel glutamine-rich activation motif. *Cell 55*, 887−898.
43. Coux, O., Tanaka, K., and Goldberg, A. L. (1996) Structure and functions of the 20S and 26S proteasomes. *Annu. Rev. Biochem. 65*, 801−847.
44. Hedgepeth, C. M., Deardorff, M. A., Rankin, K., and Klein, P. S. (1999) Regulation of glycogen synthase kinase 3beta and downstream Wnt signaling by axin. *Mol. Cell. Biol. 19*, 7147−7157.
45. Kikuchi, A. (1999) Modulation of Wnt signaling by Axin and Axil. *Cytokine Growth Factor Rev. 10*, 255−265.
46. Chida, K., and Vogt, P. K. (1992) Nuclear translocation of viral Jun but not of cellular Jun is cell cycle dependent. *Proc. Natl. Acad. Sci. U.S.A. 89*, 4290−4294.
47. Mikaelian, I., Drouet, E., Marechal, V., Denoyel, G., Nicolas, J. C., and Sergeant, A. (1993) The DNA-binding domain of two bZIP transcription factors, the Epstein-Barr virus switch gene product EB1 and Jun, is a bipartite nuclear targeting sequence. *J. Virol. 67*, 734−742.
48. Bannister, A. J., Oehler, T., Wilhelm, D., Angel, P., and Kouzarides, T. (1995) Stimulation of c-Jun activity by CBP: c-Jun residues Ser63/73 are required for CBP induced stimulation in vivo and CBP binding in vitro. *Oncogene 11*, 2509−2514.
49. Mimnaugh, E. G., Bonvini, P., and Neckers, L. (1999) The measurement of ubiquitin and ubiquitinated proteins. *Electrophoresis 20*, 418−428.
50. Bossis, G., Ferrara, P., Acquaviva, C., Jariel-Encontre, I., and Piechaczyk, M. (2003) c-Fos proto-oncoprotein is degraded by the proteasome independently of its own ubiquitinylation in vivo. *Mol. Cell. Biol. 23*, 7425−7436.

BI036256+